Available online at www.sciencedirect.com
ScienceDirect
International Journal of Thermal Sciences 47 (2008) 584–590
International Journal of Thermal Sciences
www.elsevier.com/locate/ijts

Analysis of evaporation of dense cluster of bicomponent fuel droplets in a spray using a spherical cell model

Joydeep Ghosh, Achintya Mukhopadhyay *, Gurram V. Rao, Dipankar Sanyal

Department of Mechanical Engineering, Jadavpur University, Kolkata 700 032, India

Received 4 May 2006; received in revised form 19 February 2007; accepted 7 May 2007

Available online 21 June 2007

Abstract

Evaporation of dense cluster of bicomponent fuel drops has been analyzed using a spherical cell model. The motivation of the work is to develop a droplet model that considers multicomponent and interference effects but is simple enough to be incorporated in a spray combustion code. The behaviour of the array of droplets in the spray has been analysed in terms of a unit cell, which represents the sphere of influence of the droplet. The gas-phase transport has been modelled as convective–diffusive while the liquid-phase processes as transient-diffusive. Convective heat and mass transfer condition has been used at the cell surface. Incomplete evaporation (saturation) due to accumulation of fuel vapour and complete evaporation respectively have been observed in regions of dense and dilute clusters of droplets. Close to the saturation, the evaporation from the droplet takes place at a rate comparable to the mass diffusion within the droplet.

Keywords: Dense spray; Multicomponent; Evaporation; Cell model

1. Introduction

Combustion of liquid fuel spray has been widely investigated owing to its importance in a number of devices like direct injection engines, gas turbines and propulsion systems for rockets and missiles. The behaviour of the spray depends on the evaporation and combustion characteristics of individual droplets, which are strongly influenced by the presence of neighbouring droplets. Depending on the size and number density of the droplets in the spray, the droplets may burn individually or in a group. Again, the fuels used in all these devices are blended to achieve desirable performance and emission levels.

Use of CFD for design of spray combustion devices has become fairly routine. The predictive capabilities of a spray combustion code crucially depend on the model used for evaporation of droplets. For realistic prediction, the model should incorporate both multicomponent and multi-drop features. However, the mathematical modeling of spray combustion is extremely complex, owing to the existence of a wide range of length scales. The phenomena at the droplet scale involving length scales, which are much smaller than the grid resolution of a typical CFD study, need to be described through suitable subgrid level models that capture the essential physics and yet remain computationally simple enough to be incorporated in a full-scale CFD model for spray combustion.

A powerful approach for analysing multiple droplet systems is the unit cell approach. Unlike discrete droplet models that are suitable for geometrically simple arrays of only a few droplets, this method can handle a large cloud of droplets. In this approach, the spray is divided into a number of spherical cells, each cell containing a droplet. This model has been used by a number of workers for modeling evaporation [1–11] and combustion [12,13] of droplets within a spray. An extensive review of works on droplet evaporation and combustion using spherical cell model has been presented by Mukhopadhyay and Sanyal [13]. Tishkoff [2] and Bellan and Cuffel [3] modeled evaporation of droplets in a dense spray by specifying temperature and species concentration at the edge of the cell. Bellan and Harstad [4–7] extended the model of Ref. [3] by including convective effects, heat and mass transfer from the entire cluster and electrostatic field effects. Jiang and Chiang [8–11] envisaged the spray to consist of an outer hot homogenous gaseous

* Corresponding author. Tel.: +91 33 24146177; fax: +91 33 24146532.
E-mail address: amukhopadhyay@mech.jdvu.ac.in (A. Mukhopadhyay).

1290-0729/$ – see front matter
doi:10.1016/j.ijthermalsci.2007.05.002

region enclosing a cool heterogeneous region containing the droplets. They modelled the heterogeneous region, using the 'sphere of influence' (cell) concept of Bellan and Cuffel [3]. All these works focused on evaporation of single component droplets only.

Sanyal and Sundararajan [12] extended the model of Bellan and Cuffel [3] for thin-flame combustion of single-component fuel drops in a slowly moving dilute spray and used a more general convective boundary condition at the cell surface (cell Nusselt number). Subsequently, Mukhopadhyay and Sanyal [13] improved this analysis by representing the heat and mass transfer coefficient from the cell boundary by means of a Nusselt number, determined implicitly from the solution of the transport equations. Mukhopadhyay and Sanyal [13] further incorporated the variation of ambient properties in the cell cluster due to combustion within the cells. The models of Sanyal and Sundararajan [12] and Mukhopadhyay and Sanyal [13] assume the existence of an envelope flame around each droplet. This is observed in reasonably dilute sprays at some distance from the injector. But very close to the injector, the spray is too dense to allow for droplets to burn in a discrete droplet burning mode and a group flame develops around a cluster of droplets. Rao et al. [14] developed a model for evaporation of droplets within a dense spray and identified several regimes of droplet evaporation depending on the droplet spacing. However, their work considered only single component droplets. Compared to the single component droplets, the presence of components with different volatilities is expected to significantly alter the evaporation regimes. In addition, due to reduction in evaporation rate in a dense spray, the time scales for an evaporating binary droplet in a spray would be significantly different from that of an isolated bicomponent fuel droplet. Thus the evaporation characteristics of a bicomponent fuel droplet would show significant variations from those of both isolated bicomponent droplets and single component droplets in a spray. The objective of the present work is to extend the cell model developed earlier [12–14] to study evaporation of bicomponent fuel droplets in a dense spray.

2. Physical model

The spray has been envisaged as a cluster of identical droplets, modelled in terms of a representative single droplet evaporating inside a single representative unit spherical cell inside the cluster ambient (cf. Fig. 1). Similar to the earlier models [3,12–14] the cells are assumed to touch each other. The interstitial regions between the touching spherical cells are termed as the ambient and act as common sink of fuel vapour and source of energy for all the cells in the cluster. For simplicity, the cell surface ambient condition is assumed to be identical for each cell.

3. Mathematical model

The mathematical model is similar to that of Mukhopadhyay and Sanyal [13], based on identical assumptions, which are not repeated here.

The mathematical model presented here consists of the following sets of equations: vapour phase equations, liquid phase equations, interface equations and equations for temporal variation of ambient conditions.

3.1. Vapour phase equations

The vapour phase equations are identical to those presented in Ref. [13] for the inner (fuel) region. However, since there is no flame in the present model, this region extends up to the cell boundary.

3.2. Liquid phase and interface equations

The transient diffusive transport equations and initial and boundary conditions for energy and species in the liquid phase,

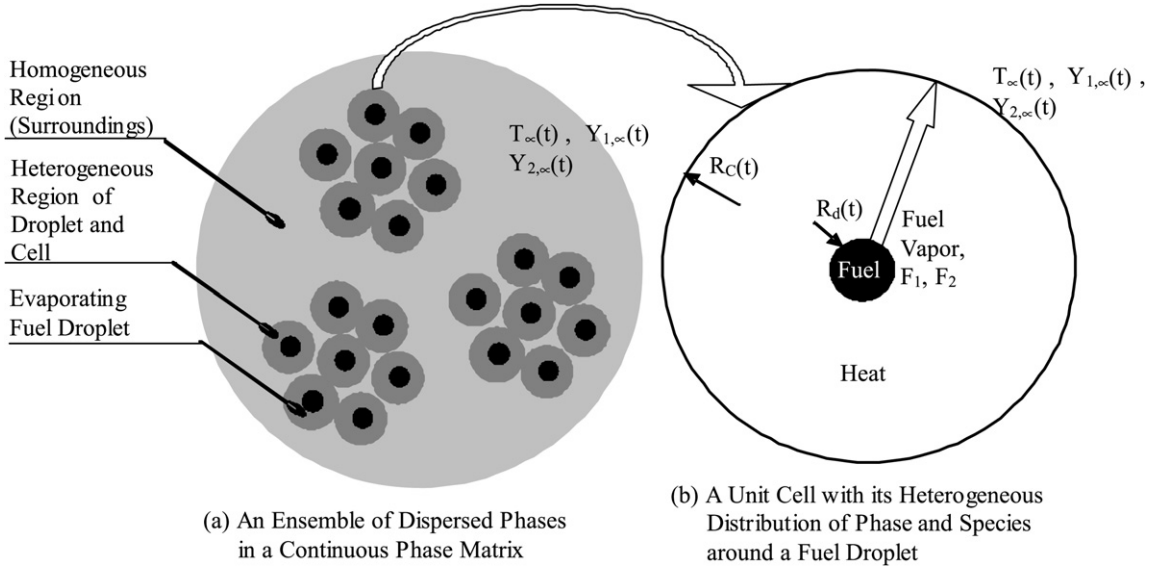

Fig. 1. Schematic of spray evaporation and unit cell modeling.

the temperature and concentration gradients at the interface on the liquid side and the rate of droplet surface regression are identical to those in Ref. [15] and not repeated here for brevity.

3.3. Cell boundary conditions

In the present work, the convective type cell boundary conditions have been adopted from Sanyal and Sundararajan [12] and Mukhopadhyay and Sanyal [13]. The rationale for choice of such boundary conditions is discussed in Ref. [13]. However, the current model admits the presence of each component of fuel vapour in the interstitial region, as would be encountered near the core of a spray or in fuel-rich pockets generated due to local extinction in turbulent flames. Following [12,13], we obtain an estimation of cell Nusselt number by solving an auxiliary heat and mass transfer problem for an isolated sphere in a quiescent infinite ambient. This approach of determining the Nusselt number by considering a single cell is consistent with the superposition technique of Labowsky [16] and point source method of Annamalai et al. [17]. The collective influence of multiple cells exchanging heat and mass with the same ambient is accounted for through the temporal variation of ambient conditions, as discussed below. The details of the derivation are available in Rao [18].

3.4. Determination of temporal rate of variation of ambient conditions

The temporal rates of accumulation of fuel vapour in the ambient and decrease of ambient temperature due to evaporation within each cell are determined by mass and energy balance in the region outside the cells following the procedure of Ref. [13]. The only difference is that in the present case, the fuel vapour is transported across the cell boundary unlike the combustion model of Ref. [13] where oxygen is transported. The algebraic details are available in Rao [18]. The values of temperature and fuel mass fraction at the cell surface are expressed in terms of the surface parameters using gas phase solution.

3.5. Temporal variation of pressure and cell radius in the gas phase

Due to variation of ambient temperature and change in the total gas content of the ambient, either or both of cell radius and gas phase pressure may change. As a consequence of neglecting fuel vapour accumulation within the cell, the mass inside the cell remains constant. Hence, the entire mass build-up due to vaporisation takes place in the ambient region only. The temporal variation of the cell radius is obtained following the approach of Mukhopadhyay and Sanyal [19].

Although the model can handle temporal variation of both ambient pressure and cell volume, in the present work, all results are presented assuming gas phase pressure to remain constant with time. Thus the cell radius alone varies temporally.

4. Solution procedure

At any time step, using the values of temperature and mass fraction at the droplet surface, the gas phase equations are solved analytically. This solution is used to calculate the interface conditions, which form the boundary conditions for the liquid phase equations. The liquid phase equations are solved numerically using control volume method. The solution of the liquid phase equations yield the surface parameters for the next time step. The converged values at a given time step are used to calculate the Nusselt number and ambient conditions for the next time step. The calculations are terminated when the droplet diameter falls below 10% of its initial value. Further details of the solution procedure are available in Rao [18] and Mukhopadhyay and Sanyal [13].

5. Results and discussions

5.1. Validation

The code has been validated in our earlier work [15] for isolated bicomponent droplets. We did not find any experimental or theoretical results for validating the predictions for evaporation of bicomponent fuel droplets in a dense spray. Consequently, the cell model was validated against experimental results for evaporation of single component droplets in a dense spray [20]. Fig. 2 shows the results for evaporation of a dense spray of tetralin droplets in nitrogen [20] in terms of the fraction of the original droplet volume remaining in liquid state. The initial values for droplet diameter, droplet temperature and ambient temperature are 30 μm, 38 °C and 75 °C respectively. The thermophysical properties listed in Ref. [20] have been used in the simulation. Fig. 2 shows that for both the cell radii, the model predictions agree very well with the experiments qualitatively and quantitatively. In Ref. [20], the droplet density in the spray has been characterized in terms of number density of the droplets. The corresponding values of cell radius used

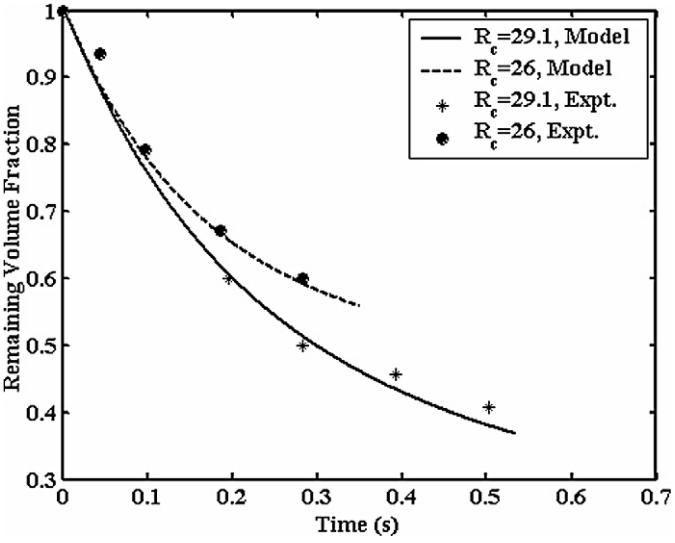

Fig. 2. Validation of cell model results with experiments [20].

for the validation are obtained using the procedure outlined in Ref. [13]. It may be noted that the dimensionless droplet spacing listed in Ref. [20] is computed on the basis of a different packing model (simple cubic) which gives a different packing efficiency compared to the Face-Centred Cubic arrangement used in Refs. [3,12,13] and adopted in the present work.

5.2. Characteristics of bicomponent spray evaporation

The results presented here in the following pages are for droplets of binary mixtures of heptane and hexadecane. All results correspond to a composition of 99% heptane and ambient pressure and temperature of 1 bar and 1000 K respectively. The choice of the composition of the droplet is guided by our earlier observation [15] that binary characteristics are most distinctively observed when the component with higher boiling point is added in small quantities. The results are for a constant ambient pressure.

In this paper, temperature has been non-dimensionalised using a scale of L_1/C_p, where L_1 and C_p represent the latent heat of the volatile species (heptane) and gas phase average specific heat, for which the reference temperature (L_1/C_p) is 142.04 K. Thus the dimensionless values of the normal boiling points of the two fuel components, heptane (normal boiling point, 371.6 K) and hexadecane (normal boiling point, 560 K) are 2.616 and 3.942 respectively. Time has been normalised with the gas phase mass diffusion time at ambient conditions, $r_{d,0}^2/D_\infty$, where $r_{d,0}$ and D_∞ represent the initial droplet radius and gas phase mass diffusivity at ambient temperature respectively, the values of which are taken as 30 μm and 2.47×10^{-5} m^2/s. The reference timescale is, therefore, 3.64×10^{-5} s.

Fig. 3 shows the temporal variation of square of the droplet radius for different values of cell radius. The cell radius can be related to average spacing between the droplets or number density of droplets in the spray. Assuming equal separation between droplets in a cluster, the cell diameter becomes equal to the spacing between the droplets. Alternatively, the cell radius

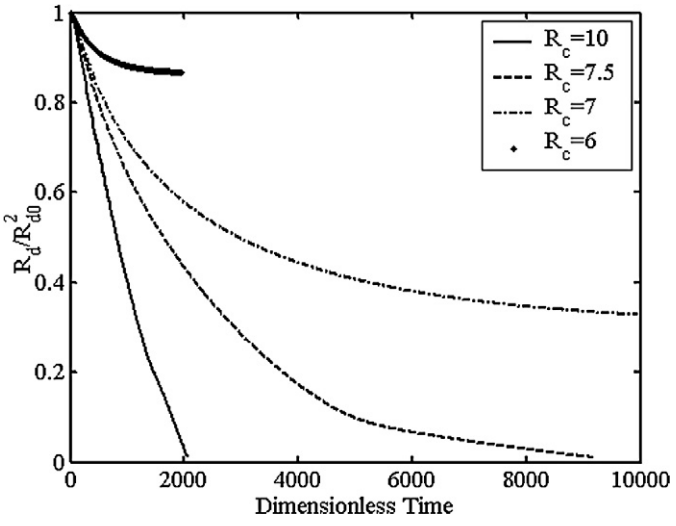

Fig. 3. Effect of cell radius on droplet life.

can be evaluated in terms of number density of droplets in the spray (V/N). In the adopted model, the pressure inside the cell remains constant. Consequently, the cell radius grows due to accumulation of fuel vapour. The thermophysical properties have been evaluated using correlations in Reid et al. [21]. At low values of initial cell radius ($R_c = 6, 7$), complete evaporation of droplets does not take place due to accumulation of fuel vapour in the interstitial region while at higher radii, complete evaporation is observed. A similar observation was reported by Rao et al. [14] in the context of single component droplets. Following Tishkoff [2], this cessation of evaporation has been termed "saturation". This incomplete evaporation is a unique feature of droplets in a dense spray. At higher cell radii, $R_c > 7$, the interference effects are weaker and hence complete evaporation takes place. In this regime, two distinct slopes, characteristic of binary droplets with components with widely differing volatilities, are observed. However, although the two slopes are constant at $R_c = 10$, at $R_c = 7.5$, there is a significant nonlinearity in the curve, caused by accumulation of the fuel vapour.

Fig. 4(a) shows the variation of droplet surface temperature at different cell radii. At $R_c = 6$, the saturation is achieved very early in the droplet life. During this short span, the lower boiling point component is the major evaporating species. Consequently, the surface temperature remains close to but less than the boiling point of the more volatile component, after the initial heat-up period. On the other hand, at $R_c = 10$, where two distinct d^2-law regimes are observed, the surface temperature also shows the different stages characteristic of evaporation of bicomponent droplets. At this cell radius, the temporal variation of the droplet surface temperature shows four distinct regimes: Initial heat-up period is followed by a phase of nearly constant temperature during which the volatile component predominantly evaporates. This is followed by an intermediate heat-up period, and finally another period of nearly constant temperature. During this final phase, the predominant evaporating species is the less volatile component. Consequently, the droplet surface temperature during the intermediate heat up period exceeds the boiling point of the volatile species and approaches the boiling point of the less volatile species. However, at $R_c \sim 7$, the variation of droplet surface temperature shows interesting features. At these cell radii, the final droplet temperature attains an intermediate value between the constant temperatures observed for $R_c = 10$. At $R_c = 7.5$, which represents complete evaporation but is close to the transition from saturation, an intermediate heat-up period is observed. However, such a heat-up period is absent for $R_c = 7$. This nature of variation will be explained in the following paragraphs. It may, however, be noted that the steady state values of droplet surface temperature for $R_c = 6$ and $R_c = 10$ are significantly lower than the normal boiling points of the two fuel components, unlike the case of isolated single component droplets where the steady state droplet surface temperature is slightly less than its boiling point. Since the steady state temperature depends strongly on the ambient temperature, the lower value of droplet surface temperature can be explained by the fact that in a dense spray, there is a significant cooling of the ambient even for cases of complete evaporation, as shown in Fig. 4(b). That the low final

temperature is a consequence of closely packed droplets in the spray is evident from the fact that the dimensionless droplet surface temperature increases from 2.995 for $R_c = 10$ to 3.222 for $R_c = 50$, when the evaporation characteristics are close to that of isolated droplet. The corresponding final ambient temperatures are 3.613 and 6.819 respectively. In both cases, the initial ambient temperature is 7.04.

Fig. 5 shows the variation of the liquid-side concentration of heptane at the droplet surface at different cell radii. At $R_c = 6$, where saturation is reached very early, the concentration remains close to the initial value of 0.99 till the end. At $R_c = 7$, which also represents saturation that is obtained after considerable droplet evaporation, the final concentration drops only gradually. On the other hand, for $R_c = 10$, after the first d^2-law period, the surface concentration drops sharply to a near zero value. At intermediate cell radii, the equilibrium concentration reaches intermediate values. A comparison with the previous figure reveals a direct correlation between the droplet surface temperature and the heptane concentration. The instantaneous surface temperature increases with the increase in hexadecane concentration. The surface temperature and concentration at $R_c = 7$ and 7.5 indicate that both the species simultaneously evaporate till the end. This in sharp distinction to the rapid depletion of the volatile component observed in isolated droplets [15].

The evaporation characteristics for a binary droplet are determined by the timescales of evaporation and liquid phase diffusion. The ratio of the evaporation constant to the mass diffusivity of the liquid species compares the timescales of these two phenomena. When the evaporation is much faster than the mass diffusion, the droplet surface loses the volatile component at a much higher rate than the rate at which it is transported by diffusion from the interior. This results in a gradual depletion of the volatile component from the surface. Thus at the end of the first d^2-law period, the surface becomes rich in hexadecane although the core is still rich in heptane. On the other hand,

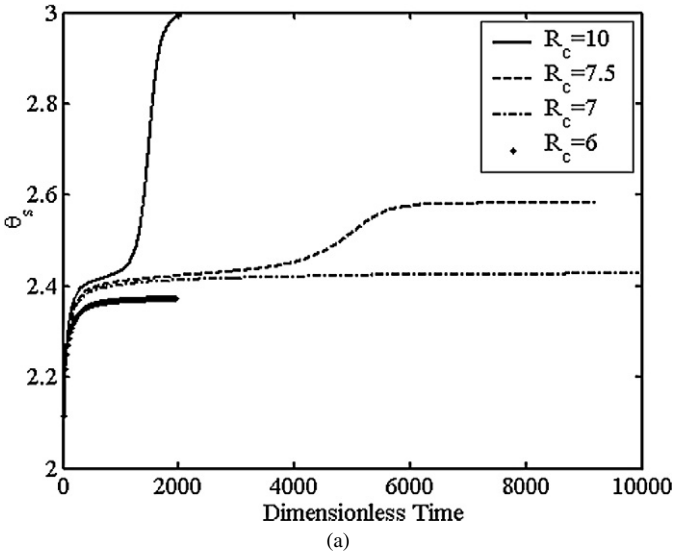

Fig. 4. Effect of cell radius on (a) droplet surface temperature and (b) ambient temperature.

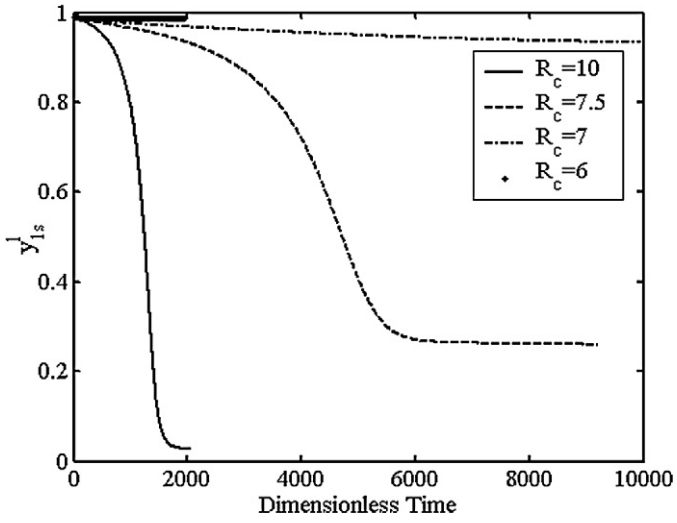

Fig. 5. Effect of cell radius on liquid heptane concentration at droplet surface.

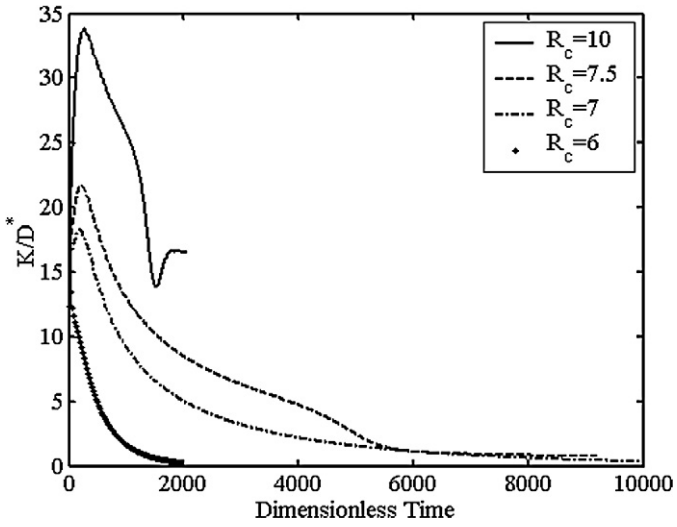

Fig. 6. Temporal variation of ratio of evaporative and diffusive timescales for different cell radii.

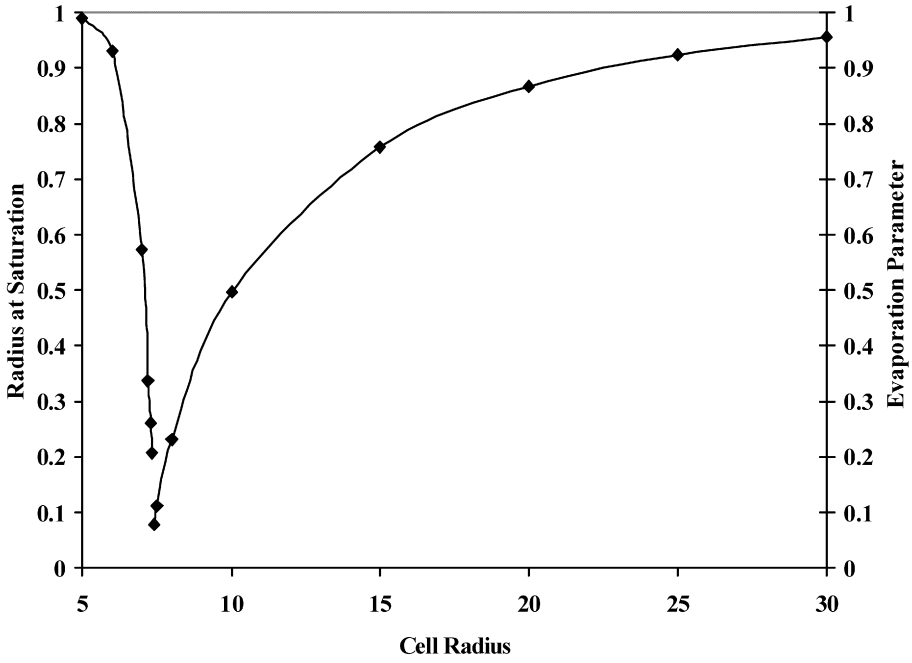

Fig. 7. Droplet radius at saturation and evaporation parameter for different initial cell radius.

when the timescales for diffusion and evaporation are comparable, the volatile component from the interior gets sufficient time to be transported to the surface. Consequently, the effect of evaporation penetrates to the interior and the surface composition represents the overall composition within the droplet.

Fig. 6 shows the variation of the ratio of the evaporation and diffusion timescales for different cell radii. It is observed that the ratio, $K/D^* \gg 1$ for $R_c = 10$ throughout the droplet life. Consequently, the high resistance to diffusion leads to depletion of heptane from the droplet surface. On the other hand, for $R_c = 7$ and 7.5, the accumulation of vapour retards the evaporation significantly. Consequently, at the later stages, the evaporation constant reduces by an order of magnitude and $K \sim D^*$. At this rate of evaporation, fuel vapour is transported to the surface from the interior at a rate comparable to that of the evaporation. Consequently, the surface retains a significant amount of heptane. At $R_c = 6$, the evaporation ceases due to saturation effect and consequently the ratio tends to zero.

Fig. 7 summarizes the different regimes of droplet evaporation in a fuel spray. At a cell radius of around 7.35, transition from saturation to complete evaporation takes place. The extent of saturation is quantified by the droplet radius at saturation. On the other hand, the interference effect of neighbouring droplets for a completely evaporating droplet is identified with the help of an evaporation parameter, which is the ratio of the time of evaporation of an isolated droplet to the time of evaporation of the droplet in the spray [2]. For saturation cases, as the cell radius increases, the attainment of saturation is delayed. This allows for greater evaporation of the droplet. Thus as the cell radius increases, the droplet radius at saturation decreases. On the other hand, the interference effects lead to a reduction in evaporation rate. Consequently, as the cell radius decreases, the droplet life increases. This leads to a decrease in the evaporation parameter with decrease in cell radius.

6. Conclusions

Evaporation of dense cluster of bicomponent droplets has been investigated. The results indicate that for very dense sprays, complete evaporation is not possible due to accumulation of fuel vapour and cooling of the ambient. The results indicate that the timescale of evaporation near saturation differs considerably from that for isolated droplets, leading to different evaporation characteristics. The evaporation characteristics of the droplet reveal strong multicomponent and interference effects. Thus both multicomponent and multi-drop effects need to be incorporated in a droplet model for spray combustion code to achieve realistic predictions.

References

[1] J.T. Zung, Evaporation rates and lifetimes of clouds and sprays in air—the cellular model, J. Chem. Phys. 46 (1967) 2064–2070.
[2] J.M. Tishkoff, A model for the effect of droplet interaction on vaporisation, Int. J. Heat Mass Transfer 22 (1979) 1407–1415.
[3] J. Bellan, R. Cuffel, A theory of non-dilute spray evaporation based upon multiple droplet interactions, Combust. Flame 51 (1983) 55–67.
[4] J. Bellan, K. Harstad, Analysis of the convective evaporation of non-dilute clusters of drops, Int. J. Heat Mass Transfer 30 (1987) 125–136.
[5] J. Bellan, K. Harstad, The details of the convective evaporation of dense and dilute clusters of drops, Int. J. Heat Mass Transfer 30 (1987) 1083–1093.
[6] J. Bellan, K. Harstad, Turbulence effects during evaporation of drops in clusters, Int. J. Heat Mass Transfer 31 (1988) 1655–1668.
[7] K. Harstad, J. Bellan, Electrostatic dispersion of drops in clusters, Combust. Sci. Tech. 63 (1989) 169–181.
[8] T.L. Jiang, W.-T. Chiang, Effects of multiple droplet interaction on droplet vaporisation in subcritical and supercritical environments, Combust. Flame 97 (1994) 17–34.

[9] T.L. Jiang, W.-T. Chiang, Droplet vaporisation in expansible dense sprays at subcritical and supercritical conditions, Atomization and Sprays 4 (1994) 523–549.
[10] T.L. Jiang, W.-T. Chiang, Vaporisation of a dense spherical cloud of droplets at subcritical and supercritical conditions, Combust. Flame 99 (1994) 355–362.
[11] T.L. Jiang, W.-T. Chiang, Transient heating and vaporisation of a cool dense cloud of droplets in hot supercritical surroundings, Int. J. Heat Mass Transfer 39 (1996) 1023–1031.
[12] D. Sanyal, T. Sundararajan, An analytical model of spray combustion for slowly moving fuel drops, Int. J. Heat Mass Transfer 35 (1992) 1035–1048.
[13] A. Mukhopadhyay, D. Sanyal, A spherical cell model for multicomponent droplet combustion in a dilute spray, Int. J. Energy Res. 25 (2001) 1275–1294.
[14] G.V. Rao, A. Mukhopadhyay, D. Sanyal, Analysis of Evaporation of Dense Cluster of Fuel Drops using Cell Method, Proc. 6th ISHMT–ASME Heat and Mass Transfer Conference and 17th National Heat and Mass Transfer Conference, Kalpakkam, India, 2004.
[15] A. Mukhopadhyay, D. Sanyal, A study of thin-flame quasisteady spherisymmetric combustion of multicomponent fuel droplets: Part I. Modelling for droplet surface regression and non-unity gas-phase Lewis number, Int. J. Energy Res. 23 (1999) 963–977.
[16] M. Labowsky, The effect of nearest neighbour interactions on the evaporation rate of cloud particles, Chem. Engrg. Sci. 31 (1976) 803–813.
[17] K. Annamalai, W. Ryan, S. Chandra, Evaporation of multicomponent drop arrays, Trans. ASME J. Heat Transfer 115 (1993) 707–716.
[18] G.V. Rao, Modelling of liquid fuel evaporation in a non-dilute spray, M.M.E. Thesis, Mech. Engrg. Dept., Jadavpur University, Kolkata, 2000.
[19] A. Mukhopadhyay, D. Sanyal, A parametric study of burning of multicomponent droplets in a dilute spray, Int. J. Energy Res. 25 (2001) 1295–1314.
[20] S.-C. Wong, J.-C. Chang, Evaporation of non-dilute and dilute monodisperse droplet clouds, Int. J. Heat Mass Transfer 35 (1992) 2403–2411.
[21] R.C. Reid, J.M. Prausnitz, B.E. Poling, The Properties of Gases and Liquids, fourth ed., McGraw-Hill Book Company, New York, 1988.